This is an *Accepted Manuscript*, which has been through the Royal Society of Chemistry peer review process and has been accepted for publication.

Accepted Manuscripts are published online shortly after acceptance, before technical editing, formatting and proof reading. Using this free service, authors can make their results available to the community, in citable form, before we publish the edited article. We will replace this *Accepted Manuscript* with the edited and formatted *Advance Article* as soon as it is available.

You can find more information about *Accepted Manuscripts* in the **Information for Authors**.

Please note that technical editing may introduce minor changes to the text and/or graphics, which may alter content. The journal's standard **Terms & Conditions** and the **Ethical guidelines** still apply. In no event shall the Royal Society of Chemistry be held responsible for any errors or omissions in this *Accepted Manuscript* or any consequences arising from the use of any information it contains.

Journal Name

ARTICLE

Raman microimaging of murine lungs: insight into the vitamin A content

K. M. Marzec,*[1] K. Kochan,[1,2] A. Fedorowicz,[1] A. Jasztal,[1] K. Chruszcz-Lipska,[3] J. Cz. Dobrowolski,[4,5] S. Chlopicki,[1,6] M. Baranska[1,2]

The composition of mice lung tissue were investigated using Raman confocal microscopy with 532 nm excitation wavelength supported with different experimental staining techniques as well as DFT calculations. This combination of experimental and theoretical techniques allows for the study of the distribution of lung lipofibroblasts (LIFs), rich in vitamin A, as well as the chemical structure of vitamin A. The comparison of the Raman spectra derived from LIFs with the experimental and theoretical spectra of standard retinoids showed the ability of LIFs to store all-*trans* retinol, which is partially oxidized to all-*trans* retinal and retinoic acid. Moreover, we were able to visualize the distribution of other lung tissue components including surfactant and selected enzymes (lipoxygenase/glucose oxidase).

1. Introduction

The group of retinoids, which includes retinol, retinal, retinoic acid, retinyl esters and derivatives of these structures, is collectively recognized as vitamin A or vitamin A metabolites. The use of retinoids in prevention of diseases is well documented in animal models as well as in clinical trials[1,2]. Recently number of reports suggested the role of vitamin A in the regulation of lung development and integrity. Indeed, tretinoin, also known as all-*trans* retinoic acid, an active metabolite of vitamin A, regulates lung morphogenesis and development[3] as well as the homeostasis in prenatal, neonatal and early postnatal stages[4]. It was also recently reported that retinoic acid stimulates immature lung fibroblast growth *via* a platelet-derived growth factor (PDGF)-mediated autocrine mechanism[5]. Retinoic acid and other substances belonging to the vitamin A group act synergistically to increase the content of lung retinal esters during normoxia and reduce hyperoxic lung injuries in newborn mice[6]. The importance of this group of compounds has also been evidenced in mature organisms. Studies have shown that prenatal retinoid deficiency leads to airway hyperresponsiveness in adult mice[7]. Retinoic acid can also induce alveolar repair in adult rats with elastase-induced emphysema, partially cure emphysema in tight-skin mouse mutants, and improve

dexamethasone-impaired alveologenesis in adult mice outside the temporally restricted period of alveologenesis[8-10]. All-*trans*-retinoic acid has also been proven to induce repairs in the lung of adult hyperoxic mice, reducing transforming growth factor- β1 (TGF- β1) mediated abnormal alteration[4].

Even though there are myriad reports which present the impact of exogenous retinoids on lung development and its alternations, there is a limited amount of research focused on the behavior of their endogenous content. It is known that the lung lipid interstitial fibroblasts (LIF, also referred to as lipocytes, Ito cells, vitamin A-storing cells) are capable of converting retinol to an acidic retinoid[11,12] and are involved in rodent lung development, homeostasis, and its injury/repair. Only a few years ago, the presence of lipofibroblasts in the human lung was clearly demonstrated with the use of morphological, molecular and functional characterization[13]. Such vitamin A-storing cells play a critical role in alveolar development by coordinating lipid homeostasis, *de novo* synthesis of surfactant phospholipids[14,15], retinol oxidation, and the production of more biologically active metabolites[11].

This work presents a series of morphological, biochemical and molecular investigations of the vitamin A content in LIFs in mice

Analyst Accepted Manuscript

lung tissue. The combination of the methods used allowed us to demonstrate the distribution of vitamin A, pulmonary surfactant and selected enzymes (lipoxygenase/glucose oxidase) inside lung tissue. The comparison of Raman spectra of vitamin A-storing cells with the experimental and theoretical spectra of standard retinoids, demonstrated that LIFs are able to accumulate retinol and induce oxidation and isomerization of retinoids.

2. Materials and methods

2.1. Tissue preparation and histological staining

The lungs were isolated from C57BL/6J mice (N=5) and mounted in isolated lung setup (HSE) as described elsewhere[16]. During isolation the lungs were perfused with constant flow (1.2 ml/min) with buffer (albumin 4%, HEPES 0.3% dissolved in Dulbecco's Modified Eagle Medium) and ventilated with positive pressures to keep tidal volume close to 0.2 ml. After 10 minutes of washing out (to remove the most of the blood cells from pulmonary circulation) the lungs were fixed with 4% buffered formalin *via* trachea (15 minutes), removed from thorax with heart *en block* and sunk in 4% buffered formalin for 6 hours. After fixation, they were mounted for the next 6 hours in a tissue freezing medium (Leica, Germany) with distilled water (1:1) and finally embedded in the Optimal Cutting Temperature (OCT) medium and frozen at -80°C. The measurements were performed on several cross-sections of lungs taken from the middle section of the organ (at the hilum level). The 5 μm thick cross section slides of lungs were put on CaF_2 slides. For reference, lung tissues were stained with the hematoxylin and eosin (H&E) staining method which permitted the visualization of the morphology and cellular heterogeneity of the tissue. The Martius, Scarlet Red and Methyl Blue method (MSB) was used for the connective tissue visualization, while the Oil Red O (ORO) to present the fraction of lipids. All investigations presented in this work conforms with the Guide for Care and Use of Laboratory Animals published by the US National Institutes of Health and the experimental procedures used in the present study were approved by a local Animal Research Committee (permit no 53/2009).

2.2. Raman measurements and analysis

The Raman measurements of tissue were recorded using a WITec confocal CRM alpha 300 Raman microscope (Jagiellonian Centre for Experimental Therapeutics – JCET, Krakow). The spectrometer was equipped with an air–cooled solid–state laser operating at 532 nm and a CCD detector, cooled to –60°C. The laser was coupled to the microscope *via* optical fiber with a diameter of 50 μm. A dry Olympus MPLAN (100x/0.90NA) objective was used. The scattered radiation was focused on a multi–mode fiber (50 μm diameter) and a single monochromator (focal length of 300 mm and aperture ratio equal to f/4). The monochromator of the spectrometer was calibrated using radiation from a calibrated xenon lamp (Witec UV-light source). Additionally, standard alignment procedure (single point calibration) was performed before measurement with the use of the Raman scattering line produced by a silicon plate (520.5 cm^{-1}). The integration time for a single spectrum was 0.3 s and the spectral resolution equaled 3 cm^{-1}. Raman measurements and data analysis were performed using WITec software (WITec Plus). All Raman maps based on the integration of marker bands presented in this work were obtained from the band area above the background without any spectra pre–processing. The areas above the straight line appointed between two frequencies of the beginning and the end of the spectral region of the specific band were measured. Cluster analysis presented in this work (Figures 1D and 3) was always carried out after cosmic spike removal and background subtraction (2nd order, polynomial in the spectral region of 100-3500 cm^{-1}). K – Means Clustering (KMC) in the Manhattan-distance formulation was used.

The following standard substances, supplied by Sigma-Aldrich were measured using 532 nm wavelength (catalog number in parentheses): hemoglobin from bovine blood (08449), retinol (95144), all trans-retinal (R2500), retinoic acid (R2625), oleic acid (O1008)**,** L-α-Phosphatidylcholine from egg yolk, lyophilized powder (P3556), glucose oxidase from *Aspergillus niger*, lyophilized powder, (G7141), lipoxidase from Glycine max, soybean, lyophilized powder (L7395). The measured glucose oxidase is a dimer, which consists of 2 equal subunits, each containing one flavin adenine dinucleotide (FAD) moiety and one iron. The soybean lipoxidase enzyme is also a non-heme iron enzyme which catalyses the dioxygenation of arachidonic acid and linoleic acid.

2.3. DFT calculations

Density functional theory (DFT) calculations were carried out using the Gaussian 09 program package[17] to support the analysis of experimental spectra. The geometries of the biologically active isomers of retinol, retinal and retinoic acids were fully optimized by using the 6-31G(d,p) basis set at the B3LYP level of theory[18,19]. No imaginary frequencies were found showing that the calculated molecules are true energetic minima. Theoretical Raman intensities (I^R) were obtained from the Gaussian Raman scattering activities (S) according to the expression $I_i = 10^{-12}(v_0 - v_i)^4 v_i^{-1} RA(i)$ where v_0 is the excitation wavenumber (532 nm) and v_i is the calculated

wavenumber of the normal mode i[20]. Prior to the comparison of the calculated wavenumbers with the Raman counterparts the latter were scaled down by the factor of 0.978 for the fingerprint region (1800-900 cm^{-1}) to account for anharmonicity effects, basis set and electron correlation.

3. Results and discussion

3.1. Lung tissue composition assessed with Raman microimaging (RS) and histological staining

To properly visualize the morphology and cellular heterogeneity of lung tissue, different staining methods were used. Figure 1A presents the microphotographs of lung tissue stained with the H&E, which stains cells' nuclei (blue) and cytoplasm (pink). It is also possible for H&E to differentiate the class of RBCs (dark pink), however they are better visualized with the MSB method where RBCs are stained in yellow and lung cells' nuclei in red (Fig.1C). The ORO staining is commonly used to visualize fraction of lipids. Since vitamin A is present inside pulmonary cells rich in lipids, it will be also stained

with this method. However, not all lipid-rich cells contain vitamin A. That is why, even ORO staining stood as a reference method for vitamin A-containing cells, other lipid components of lungs may interfere with the results. Lipofibroblasts, which contain vitamin A, are also rich in numerous lipid droplets containing triglycerides and other lipids. Moreover, such lipids can be transferred from LIFs to the pneumocyte type II cells and used in the synthesis of lung surfactant (LS)[21,22]. It is known that pneumocytes type II contain lamellar bodies, which store such surfactant. LS, which have lipidic characteristics, are necessary to reduce surface tension in lungs, however they do not stain with ORO. Previous studies showed that LS consist of phosphatidylcholine (main fraction), phosphatidylglycerol, phosphatidylethanolamine, cholesterol[23] as well as glycerophosphoglycerol and glycerophosphoinositol[24]. However, this composition may be changed by various factors and diseases.
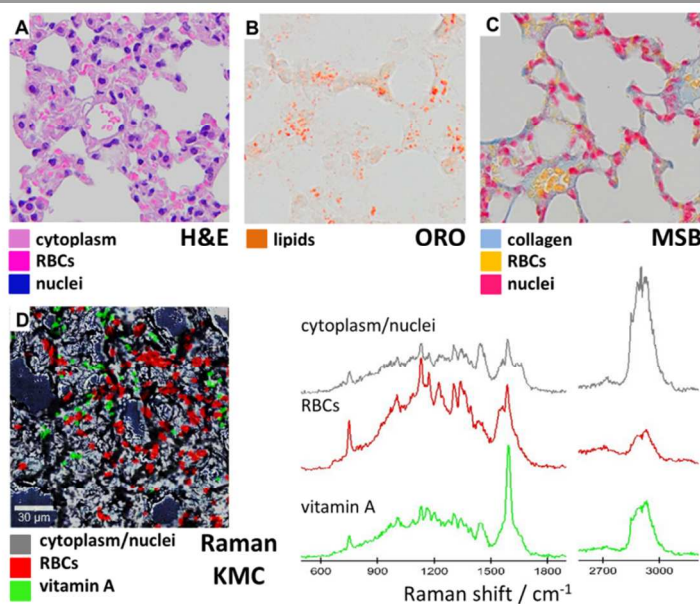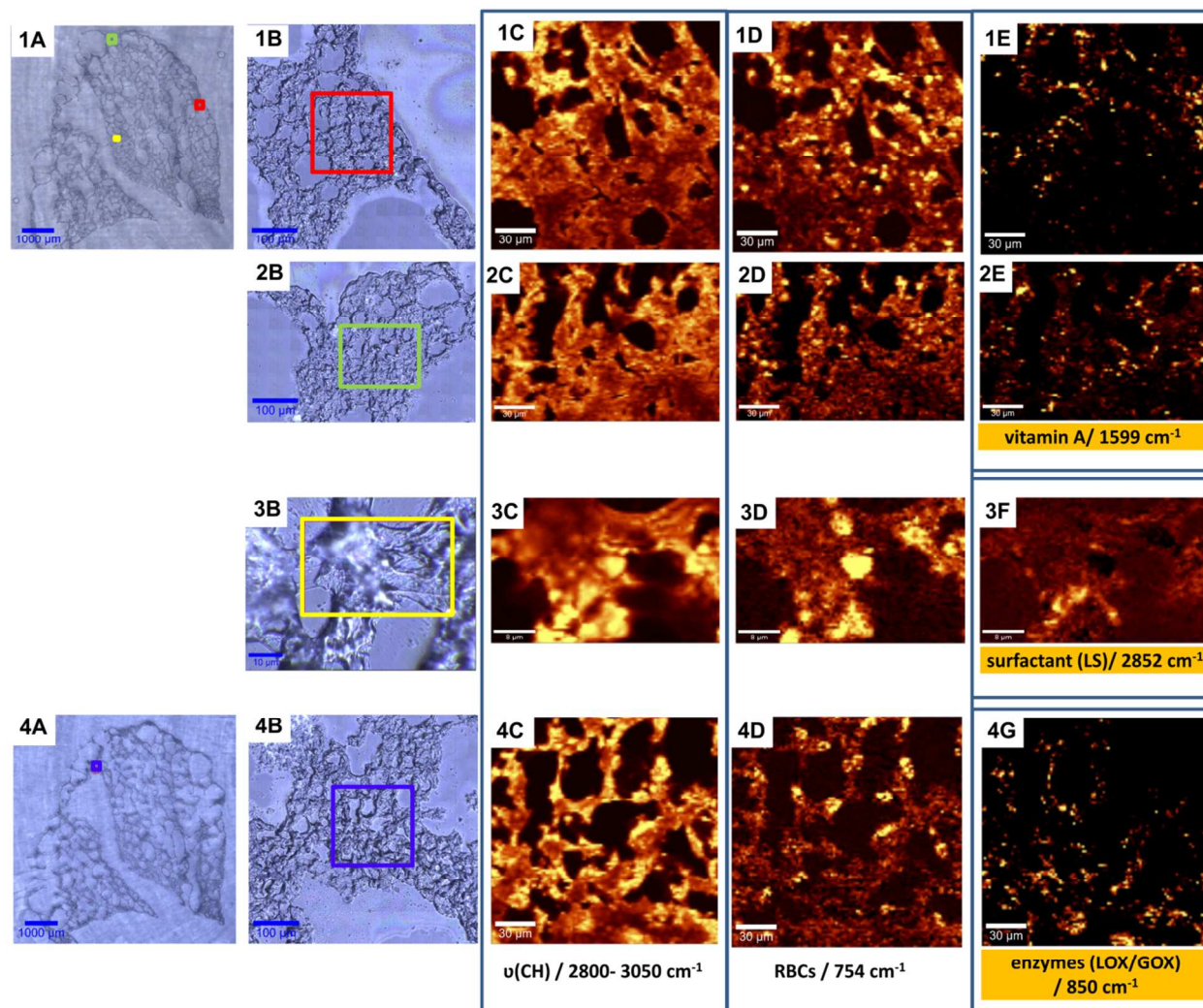

Figure 1. A microphotograph (x40) of a cross section of a middle section of lungs stained with (**A**) the hematoxylin and eosin (H&E), (**B**) the Oil Red O (ORO), and (**C**) the Martius, Scarlet Red and Methyl Blue method (MSB). (**D**) The KMC results: distribution of the 3 main classes and their average Raman spectra.

Reassuming, ORO may stain the lipid droplets in LIFs containing or not vitamin A, as well as lipids which were transferred to pneumocytes type II. Because pneumocytes type II are minor in number, we can assume that ORO staining provides information mainly about the presence of LIFs. Lipids, which are stained with ORO, constitute a large part of the cytoplasm of cells in the lung tissue. This can be observed in Figure 1B. More examples of ORO and H&E staining of mice lungs, which confirm the presence of lipid

droplets, are presented in Figure 1S (Supplementary Materials). Raman microimaging was applied to detect and differentiate between lung tissue rich in vitamin A (Figure 1D) and the other lipid components. Raman images of the lung tissue enable the detection of different components within a specified area (see Figure 2). For all of the imaged parts of lung tissue (Figure 2), the integration over the CH stretching region was carried out first (maps 1-4E). Such integration allows the visualization of the distribution of the sum of

all organic components (signal from tissue). Within this area we were able to detect various tissue components like red blood cells (RBCs), lung surfactant (LS), selected enzymes (lipoxygenase/glucose oxidase) and vitamin A. Detection of all components was made possible through the use of integration over the specific marker bands (Figure 2) as well as with the use of k-

means cluster analysis (KMC) (Figure 3). The average Raman spectra of obtained classes as well as single Raman spectra extracted from the high concentration of RBCs, LS, enzymes and vitamin A, were compared with the Raman spectra of the standard compounds and presented in Figure 3.

Figure 2. (1&4A) Microphotographs of the cross sections of a middle part of lungs taken from a control mouse with the (1-4B) labeled investigated area. **Raman mapping**: Integration maps of: (C) CH stretching band approx. in the region 2800-3020 cm^{-1} (organic matter), (D) a band centered at 1130 cm^{-1} or 745 cm^{-1} (Hb inside red blood cells-RBCs), (E) a band centered at 1598 cm^{-1} (vitamin A), (F) a band centered at 2852 cm^{-1} (lung surfactant, LS) and (G) a band centered at 850 cm^{-1} (lipoxygenase, LOX or/and glucose oxidase, GOX). The yellow color corresponds to the highest relative intensity of the integrated band or distribution of compound/group of compounds. Raman measurements for the fragments presented in Figures were carried out with a sampling density of 1.7 µm (for row 3 it was 0.5 µm). The single spectra extracted from the tissue with high concentration of vitamin A, LS enzymes and Hb compared with spectra of standard compounds are presented in Figure 3.

Interestingly, even when lungs were washed with buffer before fixation, the tissue still contained some RBCs (for all measured samples). To image RBCs inside the tissue we used the integration of the band at 750 cm^{-1}, which corresponds to the

v_{15} mode (pyrrole breathing, in plane stretching)[25] (Figure 2, maps 1D-4D). The average Raman spectrum of RBCs' class (red class, Figure 3) and a single Raman spectrum extracted from RBC agree with the spectrum of hemoglobin (Hb, Figure

3D). The higher contribution of the CH stretching bands (2800-3050 cm^{-1}) in the case of RBCs class compared to spectrum of pure Hb is connected with the presence of additional proteins and some other lung components (cytoplasm and nuclei of lung cells).

Although the KMC results were carried out after background removal, cluster mean spectra of Hb have a substantial background. Such remaining backgrounds may originate from the strong resonance enhancement of the Raman signal of Hb, as the use of the excitation wavelength of 532 nm is in resonance with the electronic transitions of Hb. On the other hand, the use of this excitation wavelength also has an effect on the observation of the pre-resonance Raman spectrum of retinols. Contrary to Hb, additional background is not observed in the class of vitamin A. This suggests, that there is an additional factor in the background increase in the case of Hb class. It was previously reported that heme inside RBCs, converts absorbed photons into heat and therefore generates a strong photothermal signal, which may have an impact on the additional increase of Hb background[26].
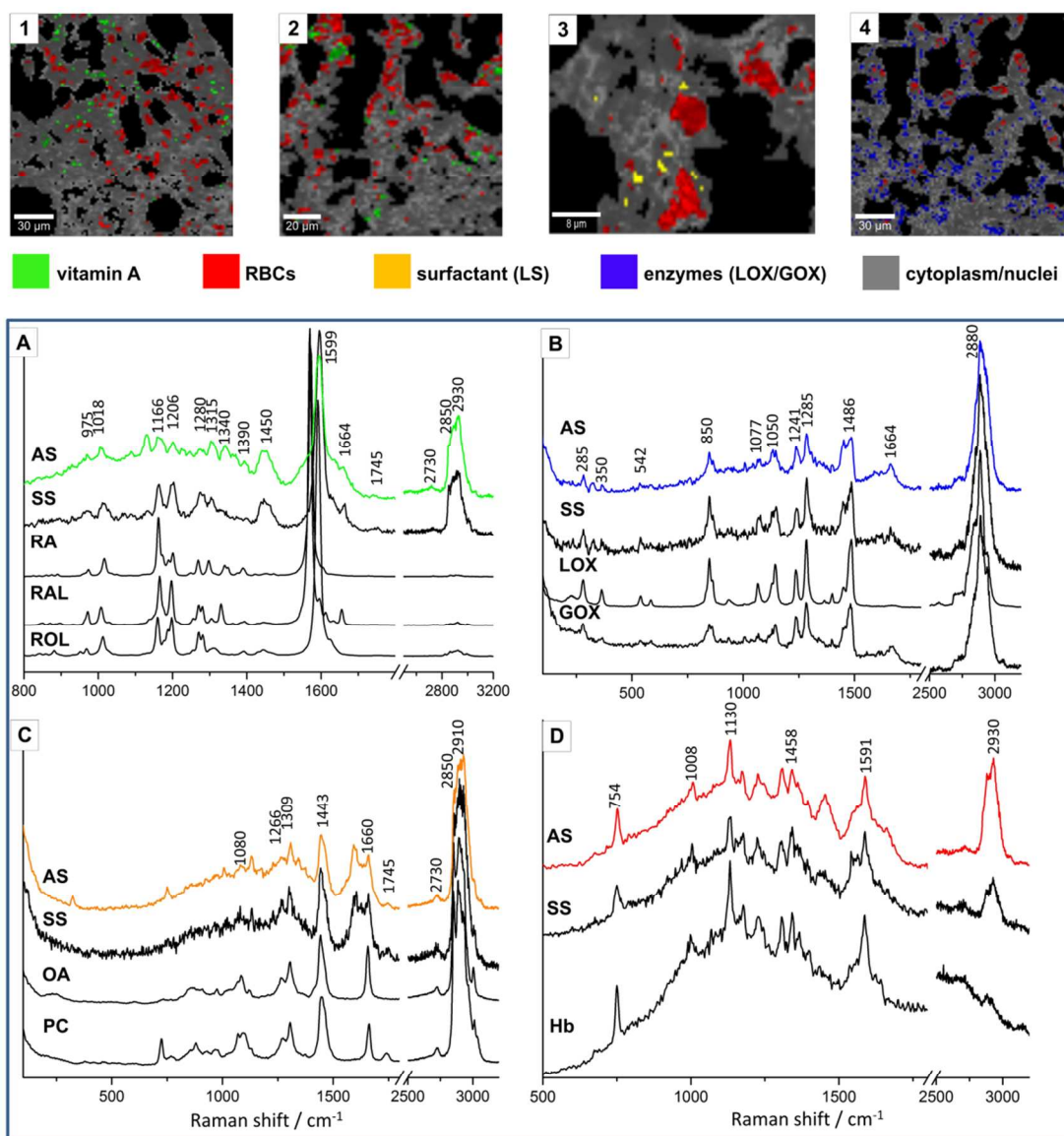

Figure 3. The KMC results for four areas of the lung tissue presented in Figure 2 with the main classes. Classes include vitamin A (green), RBCs (red), lung surfactant (yellow), enzymes (blue) and the class of cytoplasm and nuclei (grey). Black class corresponds to substrate signal and is removed as outliers. The average spectra (AS) of the respective main classes of tissue obtained from the K-means clustering were compared with the single Raman spectra (SS) extracted from lung tissue from high concentration of each class and Raman spectra of

the standard compounds: retinoic acid (RA), retinal (RAL), retinol (ROL), lipooxygenase (LOX), glucose oxidase (GOX), hemoglobin (Hb), oleic acid (OA) and L-α-phosphatidylcholine (PC).

Raman maps 1E and 2E, obtained by the integration at around 1599 cm^{-1} (marker band of vitamin A), are in agreement with the images of ORO staining. The size and distribution of the vitamin A droplets correspond to those observed in ORO staining. This is in agreement with previous studies showing that vitamin A is mainly located in lipid droplets of LIFs[11,12]. The average Raman spectrum of vitamin A class (green class, Figure 3) as well as single Raman spectrum extracted from LIFs (Figure 3A) correspond to the combination of the spectra of retinol (ROL), retinal (RAL) and retinoic acid (RA). However, there is a noticeable difference between the spectral profile of the average Raman spectrum of vitamin A class and a single vitamin A spectrum extracted from the tissue. This suggests differences in the composition of vitamin A within the measured tissue and may be connected with different oxidation state of retinoids. To study this aspect, the detailed analysis of the most intensive single spectra extracted form LIFs were

carried out with the support of DFT calculations, which is presented below (see section 3.2.).

The lipid fraction connected with the presence of lung surfactant (LS) in the lung tissue was possible to detect with the use of Raman spectroscopy when higher special resolution was used (Figure 2, map 3F). The average Raman spectrum of the lipid-rich class (yellow class, Figure 3) as well as a single Raman spectrum extracted from lipid-rich parts of tissue (Figure 3C) correspond to the spectrum of fatty acids (for example oleic acid, OA) or phosphatidylcholine (PC). The typical bands can be observed at 1266, 1309, 1745 and 2850 cm^{-1}. According to previous studies, described in the introduction, such a composition suggests, that this class can be assigned to LS. As PC was found to be the major compound in LS fraction of mouse lungs, we believe that the elongated spots observed, rich in the LS, may belong to the lamellar bodies inside type II pneumocytes.
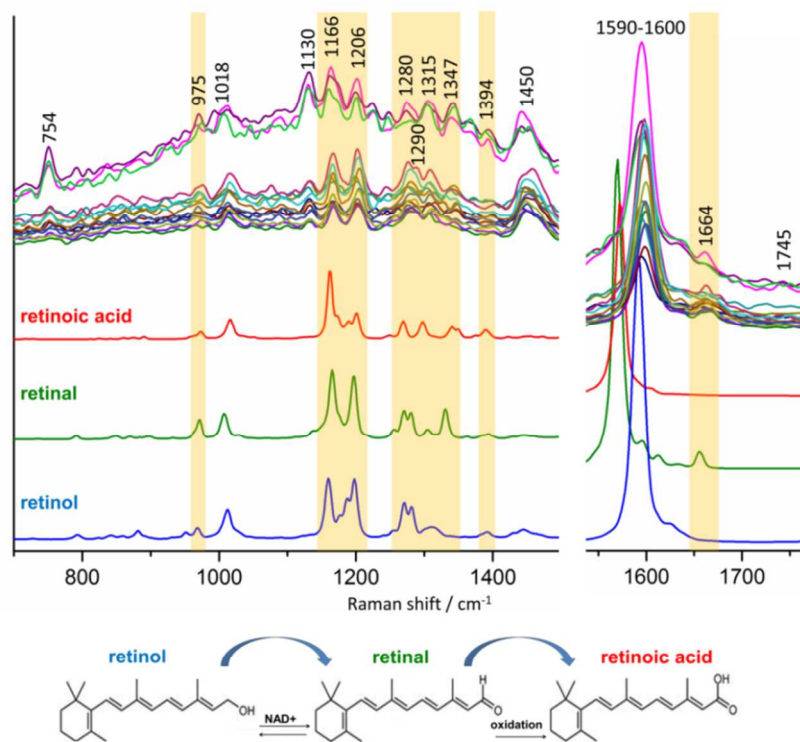

Figure 4. The single Raman spectra extracted from the lung tissue areas of high concentration of vitamin A, compared with the Raman spectra of standard compounds of all-*trans* retinol, all-*trans* retinal and all-*trans* retinoic acid.

Raman images obtained from a different lung section (Figure 2, maps 1-4) show some changes in general tissue composition.

We were able to detect either vitamin A (Figure 2, maps 1E-2E) or different groups of chemicals, which we assigned to a class

of enzymes (Figure 2, map 4G). The single Raman spectrum extracted from areas of high enzyme concentration, as well as the average Raman spectrum of the whole enzyme class (blue class, Figure 3), shows similarities to the Raman spectrum of the standard spectra of both lipoxygenase enzyme (LOX) and glucose oxidase enzyme (GOX) (Figure 3B). Single spectra of these enzymes show bands typical for proteins (amide I and III, Phe, CH-stretching region) as well as strong bands likely related to the vibrations of non-heme iron ligand. The presence of the bands at 1077 cm^{-1} and 350 cm^{-1}, along with the relative intensity of the bands at 1241 cm^{-1} to that at 850 cm^{-1}, suggest that the blue class of tissue is LOX. Even though the presence of the band at 1664 cm^{-1} in the average Raman spectrum of

enzymes class may suggest the presence of GOX, this band may also originate from the other protein signal of the tissue. If such a band would correspond to the C=C stretches in unsaturated lipids, we should also observe a band at 3012 cm^{-1} in the spectrum extracted from the tissue, which is not a case. Moreover, it was previously reported that LOX catalyses the dioxygenation of polyenoic fatty acids and its action may be affected by retinol, all-*trans*-retinoic acid and 13-*cis*-retinoic acid[27]. That fact and the profile of the Raman spectrum of observed enzymes supports that this is LOX, however further studies and immunohistochemical staining is necessary to fully confirm the origin of the spectral signal that we attributed to LOX or GOX.
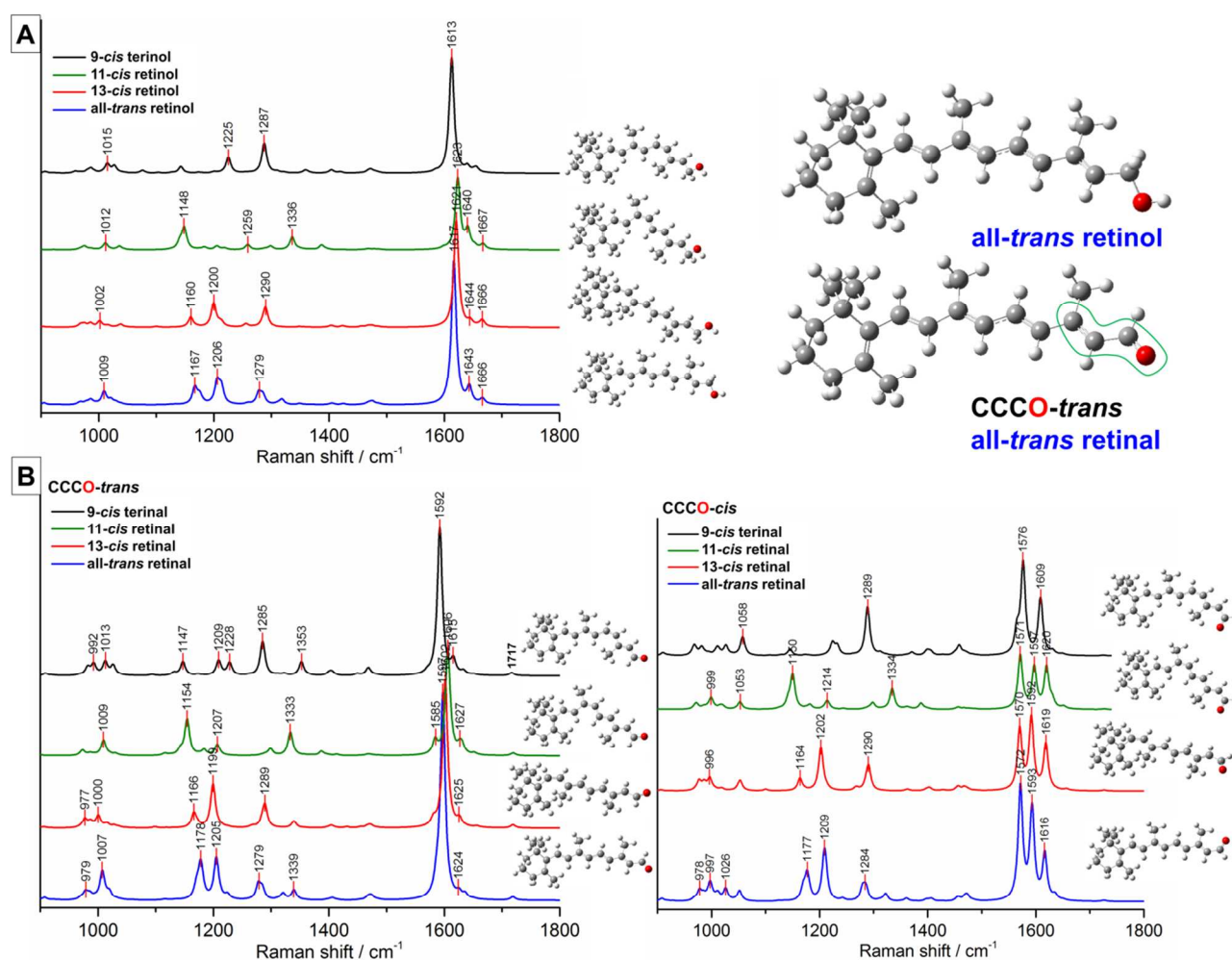
Figure 5. The theoretical Raman spectra of the biologically active isomers of (A) retinol and (B) retinal in the fingerprint region (1800-900 cm^{-1}). Spectra were simulated by the Lorentzian functions centered at the DFT(B3LYP)/6-31G(d,p) calculated wavenumbers scaled by 0.978 and with fwhm equal to 10 cm^{-1}.

3.2. Relative content of vitamin A derivatives and their isomers assessed with Raman spectroscopy and DFT

The comparison between the single Raman spectra of vitamin A extracted from different LIFs of lung tissue, with the spectra of all-*trans* retinol, all-*trans* retinal and all-*trans* retinoic acid

(Figure 4), allowed us to define the content of lung LIFs. The position of the most intensive band of the extracted spectra of vitamin A varied in the region of 1590-1600 cm^{-1}. This band corresponds to stretching vibration of the C=C bonds of four of the most common isomers of retinol, which suggests that the majority of vitamin A is in the form of retinol. The all-*trans* as well as mono-*cis* isomers of retinoids like 9-*cis*, 11-*cis* and 13-*cis* belong to the biologically active structures. It is well known that some *trans-cis* isomerization of these molecules can be found in different organ tissues[28-30]. However, the comparison of the theoretical spectra of different retinol isomers (Figure 5A) with experimental spectra extracted from the tissue indicates the presence mainly of the all-*trans* retinol.

The bands at 1664, 1347 cm^{-1} and 975 cm^{-1} in some of the extracted spectra can be assigned to the presence of retinal. Moreover, the calculations indicate that retinal occurs in the *trans* arrangement of the C=C–C=O group. In the case of theoretical spectra of retinals with the *cis* arrangement of the C=C−C=O group, the band at around 1600 cm^{-1} is spilt into doublet or triplet. This is not observed in the experimental spectra extracted from the tissue. The comparison with the theoretical spectra of different biologically active isomers with *trans* arrangement of the C=C–C=O group of retinal suggests the dominance of all-*trans* retinal (Figure 5B). Most of the spectra of the vitamin A obtained from the tissue show a doublet (or band with a shoulder) at 1280 and 1290 cm^{-1}, which suggests that spectra originate from the all-*trans* retinal and/or all-*trans* retinol. However, the presence of two single bands at 1280 and 1315 cm^{-1}, as well as the increase in intensity of the band at 1166 cm^{-1} (in some of the spectra extracted from tissue) also indicate the occurrence of retinoic acid in minor amounts.

4. Conclusions

The presented results demonstrate the capability of Confocal Raman Spectroscopy (RS) for a detailed examination of the biochemical composition of single cell type within murine lung at the molecular level. The potential of this method for such investigations enables a detailed insight into biochemical composition of these cells *in situ* inaccessible by other techniques. Confocal Raman mapping correlates to a very good extent with histological staining, which is a classic method to stain for lipids or other gross tissue constituents. However, spectroscopic results provide additional insight into the biochemical composition of various cells within the lungs. In the present work we explicitly

confirmed the presence of vitamin A within LIFs, as well as visualized lung surfactant (LS) produced by pneumocytes type II. Finally we identified selected enzymes (LOX/GOX) inside the lung places of unknown cellular origin. Accordingly, Raman spectroscopy provided the biochemical fingerprint at least of some cellular-specific areas of highly complex, multicellular lung tissue containing more than 40 types of cells. In the present work we combined the measurement results with results of DFT calculations that allowed us to conclude that within the lung tissue vitamin A is present mostly in the form of the all–*trans* retinol, although the presence of all–*trans* retinal and retinoic acid has also been detected.

Notes and references

[1] *Jagiellonian Centre for Experimental Therapeutics (JCET) Jagiellonian University, 14Bobrzyńskiego Str., 30-348 Krakow, Poland*

[2] *Faculty of Chemistry, Jagiellonian University, 3 Ingardena Str., Krakow, Poland*

[3] *AGH University of Science and Technology, Faculty of Drilling, Oil and Gas, Mickiewicza 30 Ave., 30-059 Krakow*

[4] *National Medicines Institute, 30/34 Chełmska Str., 00-725, Warsaw, Poland*

[5] *Institute of Nuclear Chemistry and Technology,16 Dorodna Str., 03-195 Warsaw, Poland*

[6] *Department of Experimental Pharmacology, Chair of Pharmacology Jagiellonian University Medical College, 16 Grzegorzecka Str., Krakow, Poland*

*email:marzec@chemia.uj.edu.pl

Acknowledgements

Analyst Accepted Manuscript

References

1   F. Alizadeh, A. Bolhassani, A. Khavari, S. Z. Bathaie, T. Naji, S. A. Bidgoli, *Int. Immunopharmacol.*, 2014, **18(1)**, 43–49.

2   K. H. Dragnev, J. R. Rigasa, E. Dmitrovsky, *Oncologist*, 2000, **5(5)**, 361–368.

3   S. Montedonico, N. Nakazawa, P. Puri, *Pediatr. Surg. Int.*, 2008, **24**, 755–761.

4   O. Kayalar, F. Oztay, *Acta Histochem.*, 2014, *doi*: *10.1016/j.acthis.2014.01.009.*

5   L. Abraham, S. Srinivasan, D. Kaetzel, M. Bruce, *Am. J. Physiol. Lung. Cell. Mol. Physiol.*, 2000, **279**, L81–L90.

6   M. L. James, A. C. Ross, A. Bulger, J. B. Philips, N. Ambalavanan, *Pediatr. Res.*, 2010, **67(6)**, 591–597.

7   F. Chen, H. Marquez, Y-K. Kim, J. Qian, F. Shao, A. Fine, W. W. Cruikshank, L. Quadro, W. V. Cardoso, *J. Clin. Invest.*, 2014, **124(2)**, 801-811.

8   G. D. Massaro, D. Massaro, *Nat. Med.,* 1997, **3**, 675–677.

9   G. D. Massaro, D. Massaro. *Am. J. Physiol. Lung Cell Mol. Physiol.*, 2000, **278**, L955–960.

10   M. Hind, A. Gilthorpe, S. Stinchcombe, M. Maden, *Thorax*, 2009, **64**, 451–457.

11   G. Dirami, G. D. Massaro, L. B. Clerch, U. S. Ryan, P. R. Reczek, D. Massaro, *Am. J. Physiol. Lung Cell Mol. Physiol.,* 2004, **286**, L249–L256.

12   A. C. Ross, *Am. J. Physiol. Lung Cell Mol. Physiol.*, *2004*, **286**, *L247–L248*.

13   V. K. Rehan, S. Sugano, Y. Wang, J. Santos, S. Romero, C. Dasgupta, M. P. Keane, M. T. Stahlman, J. S. Torday, *Exp. Lung Res.*, 2006, **32(8)**, 379-393.

14   S. E. McGowan, J. S. Torday, *Annu. Rev. Physiol.,* 1997, **59**, 43–62.

15   J. S. Torday, E. Torres, V. K. Rehan, *Pediatr. Pathol. Mol. Med.,* 2003, **22**, 189–207.

16   S. Siegl, S. Uhlig. *PLoS One*., 2012, **7(7)**, e41464, 1–11.

17   Gaussian 09, Revision D.01, M. J. Frisch, G. W. Trucks, H. B. Schlegel, G. E. Scuseria, M. A. Robb, J. R. Cheeseman, G. Scalmani, V. Barone, B. Mennucci, G. A. Petersson, H. Nakatsuji, M. Caricato, X. Li, H. P. Hratchian, A. F. Izmaylov, J. Bloino, G. Zheng, J. L. Sonnenberg, M. Hada, M. Ehara, K. Toyota, R. Fukuda, J. Hasegawa, M. Ishida, T. Nakajima, Y. Honda, O. Kitao, H. Nakai, T. Vreven, J. A. Montgomery, Jr., J. E. Peralta, F. Ogliaro, M. Bearpark, J. J. Heyd, E. Brothers, K. N. Kudin, V. N. Staroverov, R. Kobayashi, J. Normand, K. Raghavachari, A. Rendell, J. C. Burant, S. S. Iyengar, J. Tomasi, M. Cossi, N. Rega, J. M. Millam, M. Klene, J. E. Knox, J. B. Cross, V. Bakken, C. Adamo, J. Jaramillo, R. Gomperts, R. E. Stratmann, O. Yazyev, A. J. Austin, R. Cammi, C. Pomelli, J. W. Ochterski, R. L. Martin, K. Morokuma, V. G. Zakrzewski, G. A. Voth, P. Salvador, J. J. Dannenberg, S. Dapprich, A. D. Daniels, Ö. Farkas, J. B. Foresman, J. V. Ortiz, J. Cioslowski, and D. J. Fox, Gaussian, Inc., Wallingford CT, 2009.

18   C. Lee, W. Yang, R. G. Parr, *Phys. Rev. B*, 1988, **37**, 785-789.

19   A. D. Becke, *J. Chem. Phys.,* 1993, **98**, 5648-5652.

20   D. Michalska, R Wysokinski, *Chem. Phys. Lett.,* 2005, **403**, 211–217.

21   J. Torday, J. Hua, R. Slavin, *Biochim. Biophys. Acta*, 1995, **1254**, 198-206.

22   J. S. Torday, V. K. Rehan, *Am. J. Physiol.*, 2002, **283**, L130-L135.

23   R. Veldhuizen, K. Nag, S. Orgeig, F. Possmayer, *Biochim. Biophys. Acta*, 1998, **1408**, 90-108.

24   F. Basile, T. Sibray, J. T. Belisle, R. A. Bowen, *Anal. Biochem.*, 2011, **408**, 289–296.

25   A. Rygula, K. Majzner, K. M. Marzec, A. Kaczor, M. Pilarczyk, M. Baranska, *J. Raman Spectr.,* 2013, **44 (8)**, 1061-1076.

26   D. Zhang, M. N. Slipchenko, D. E. Leaird, A. M. Weiner, J-X. Cheng, *Optics Express*, 2013, **21(11)**, 13864-13874.

27   D. Goldreich, S. Grossman, Y. Sofer, E. Breitbart, D. Sklan, *Int. J. Vitam. Nutr. Res.,* 1997, **67(1)**, 4-9.

28   J. Urbach, R. R. Rando, *Biochem. J.,* 1994, **299**, 459-465.

29   P. A. Hargrave, J. H. McDowell, D. R. Curtis, J. K. Wang, E. Juszczak, S-L. Fong, J. K. M. Rao, P. Argos, *Biophys. Struct. Mech*., 1983, **9**, 235-244.

30   R. Hubbard, A. Kropf, *Ann. N.Y. Acad. Sci.,* 1958, **44**, 130-139.

Journal Name

ARTICLE

Raman microimaging of murine lungs: insight into the vitamin A content

K. M. Marzec,*[1] K. Kochan,[1,2] A. Fedorowicz,[1] A. Jasztal,[1] K. Chruszcz-Lipska,[3] J. Cz. Dobrowolski,[4,5] S. Chlopicki,[1,6] M. Baranska[1,2]

1 Jagiellonian Centre for Experimental Therapeutics (JCET) Jagiellonian University, 14Bobrzyńskiego Str., 30-348 Krakow, Poland

2 Faculty of Chemistry, Jagiellonian University, 3 Ingardena Str., Krakow, Poland. *Email:marzec@chemia.uj.edu.pl

3 AGH University of Science and Technology, Faculty of Drilling, Oil and Gas, Mickiewicza 30 Ave., 30-059 Krakow, Poland

4 National Medicines Institute, 30/34 Chełmska Str., 00-725, Warsaw, Poland

5 Institute of Nuclear Chemistry and Technology,16 Dorodna Str., 03-195 Warsaw, Poland

6 Department of Experimental Pharmacology, Chair of Pharmacology Jagiellonian University Medical College, 16 Grzegorzecka Str., Krakow, Poland

Supplementary Materials
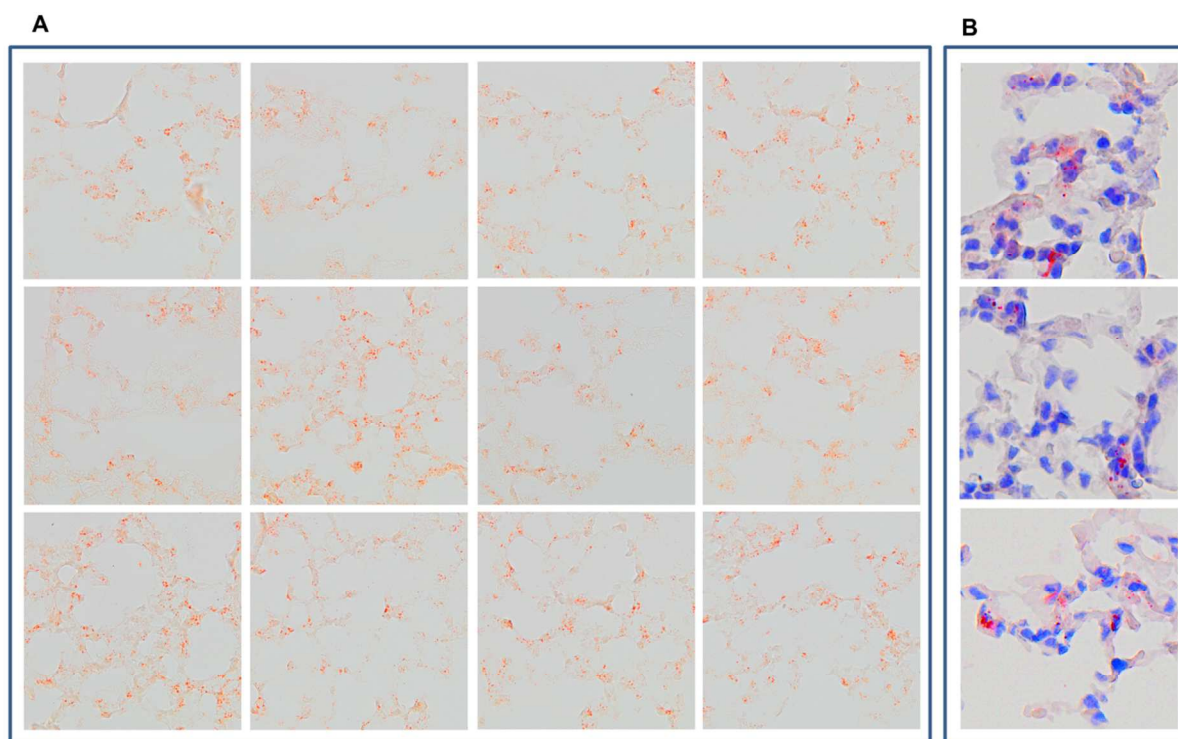
Figure S1. A microphotograph (x40) of a part of cross section of middle part of lungs of control C57 mice stained with (A) the Oil Red O (ORO), and (B) the ORO and the hematoxylin and eosin (H&E) method.